Journal of Basics and Applied Sciences Research (JOBASR)
ISSN (print): 3026-9091, ISSN (online): 1597-9962
Volume 3(6) November 2025
DOI: https://dx.doi.org/10.4314/jobasr.v3i6.30

Hydromagnetic Boundary Layer Flow of Micropolar Fluid with Multiple Slip in the Presence of Thermophoresis, Cross-diffusion, Nonlinear Thermal Radiation and Chemical Reaction

Baoku Ismail Gboyega[1*], Dahiru Jamilu[2], Bashir Sule[3] & Onifade Yemi Sikiru[4]
[1,2,3]Department of Mathematics, Federal University, Dutsin-Ma, Katsina State, Nigeria
[4]Department of Physics, Federal University of Petroleum Resources, Effurum, Delta State Nigeria.
*Corresponding Author Email: ibaoku@fudutsinma.edu.ng

ABSTRACT
A mathematical model is analyzed in order to study the heat and mass transfer characteristics in boundary layer MHD flow with multiple slip effects in a porous medium filled with a micropolar fluid. By taking into account the thermophoresis and cross-diffusion, the study considers both an artificially driven temperature jump in the opposite direction and reversed concentration jump which violate the relevant fundamental laws on thermal and concentration boundary layers. The governing partial differential equations are transformed into a set of coupled ordinary differential equations. The highly nonlinear system of ordinary differential equations are solved numerically using the sixth-order Runge-Kutta integration scheme with shooting method. The effects of various significant parameters such as Soret number, thermal radiation parameter, Dufour number, permeability parameter, Prandtl number, chemical reaction parameter, velocity slip, negative thermal and concentration slip parameters, Schmidt number and other governing parameters on the dimensionless velocity, angular velocity, temperature and species concentration profiles are presented graphically. The results indicate that the magnetic field, first order slip and porous medium parameters reduce the fluid velocity, whereas the permeability parameters have opposite effects on the velocity profile. However, decrease in porous medium parameter corresponded to a decrease in skin-friction coefficient and heat transfer's rate but increase in rate of mass transfer. Of particular interests are the non-monotonic profiles in temperature and species concentration for thermal and concentration slip parameters, which confirm nonphysicality of the negative values as experienced in electro-osmotic flows and electrochemical systems. The current results are validated with other related research work in the literature and are found to be in excellent agreement.

Keywords:
Micropolar fluid,
Thermophoresis,
Cross-diffusion,
Magnetohydrodynamics,
Velocity,
Thermal and
Concentration slips,
Nonlinearized thermal
Radiation.

INTRODUCTION

Non-Newtonian fluids with complex behaviour have been found in numerous natural and engineering systems, for example, biofluid in biological tissue and polymers as well as colloidal suspensions in engineering applications. Their experimental and theoretical investigations are central themes in rheology, shear flows and thermo-physics; are actively studied by scientists and engineers. Micropolar fluids are fluids with microstructure. They belong to a class of fluids with nonsymmetrical stress tensor that we shall call polar fluids, which could be mentioned as the well-established Navier–Stokes model of classical fluids. These fluids respond to micro-rotational motions and spin inertia and therefore, can support couple stress and distributed body couples.

Physically, a micropolar fluid is one which contains suspensions of rigid particles. The theory of micropolar fluids was first formulated by Eringen (1966). Examples of industrially relevant flows that can be studied with accordance to this theory include flow of low concentration suspensions, liquid crystals, blood, lubrications and so on. The micropolar theory has recently been applied and considered in different aspects of sciences and engineering applications [(Mirgolbabaee *et al.* 2017)].

Micropolar fluid obeys the constitutive equations of the considered non-Newtonian fluid model to analyze the behaviour of exotic lubricants, colloidal suspensions, polymeric fluid and liquid crystals.

How to cite this article: Baoku I. G., Dahiru J., Bashir S. & Onifade Y. S. (2025). Hydromagnetic Boundary Layer Flow of Micropolar Fluid with Multiple Slip in the Presence of Thermophoresis, Cross-diffusion, Nonlinear Thermal Radiation and Chemical Reaction. *Journal of Basics and Applied Sciences Research*, *3*(6), 320-332. https://dx.doi.org/10.4314/jobasr.v3i6.30

Abdulaziz and Hashim (2009) studied fully developed free convection heat and mass transfer of a micropolar fluid between porous vertical plates, in that research, they extended the work of Cheng (2006) on fully developed natural convection heat and mass transfer of a micropolar fluid in a vertical channel with asymmetric wall temperatures and concentrations, by taking the vertical plate to be porous. The resulting boundary-value problem is solved analytically by the homotopy analysis method (HAM). Profiles for velocity and microrotation are presented for a range of values of the Reynolds number and the micropolar parameter.

Boundary layers are important in many applications, such as aerodynamics, heat transfer, and fluid machinery. For example, the drag on an aircraft is largely due to the boundary layer on its surface. The boundary layer also plays a role in the design of heat exchangers and other heat transfer devices. That is why many researchers are paying more attention on it. Subhas *et al*. (2009) scrutinized the heat transfer in MHD viscoelastic boundary layer flow over a stretching sheet with non-uniform heat source/sink. Chen *et al*. (2019) studied the unsteady boundary layer flow of viscoelastic MHD fluid with a double fractional Maxwell model. Mahantesh *et al*. (2011) studied the heat transfer in MHD viscoelastic boundary layer flow over a stretching sheet with thermal radiation and non-uniform heat source/sink. Ibrahim (2016) studied the MHD boundary layer flow and heat transfer of micropolar fluid past a stretching sheet with second order slip.

Studies involved thermal radiation are carried out by many researchers such as Baoku *et al*. (2010) who studied magnetic field and thermal radiation effects on steady hydromagnetic Couette flow through a porous channel. Dulal and Chandra (2019) made a study on combined performance of non-linear thermal radiation and chemical reaction on MHD convective heat and mass transfer of a micropolar fluid over a non-isothermal surface. Vijaya *et al.* (2019) [20] studied heat transfer analysis in a micropolar fluid with non-linear thermal radiation and second-order velocity slip. Bhattacharyya *et al*. (2012) conducted a research on the effects of thermal radiation on micropolar fluid flow and heat transfer over a porous shrinking sheet.

Soret and Dufour effects are important for intermediate molecular weight gases in coupled heat and mass transfer in fluid binary systems, often encountered in chemical process engineering. Both free and forced convection boundary layer flows with Soret and Dufour have been addressed by many researchers. Pal and Das (2021) studied the Soret-Dufour magneto-thermal radiative convective heat and mass transfer of chemically and thermally stratified micropolar fluid over a vertical stretching/shrinking surface in a porous medium, where it was explored that the velocity and temperature distribution decrease with enhancement in the Prandtl number and having reverse effects on the concentration distribution. Sui *et al*. (2017) studied the influence of particulate thermophoresis on convection heat and mass transfer in a slip flow of a viscoelasticity-based micropolar fluid. Baoku *et al*. (2013) studied heat and mass transfer on a MHD third grade fluid with the effects of partial slip parameter on the flow past an infinite vertical insulated porous plate in a porous medium and pronounced the contributions of slip flow on the problem.

Also, combined heat and mass transfer problems with chemical reaction are of importance in many processes such as in the processing of chemical engineering fluids including polymeric suspensions, lubricant manufacture e.t.c. and have therefore received a considerable amount of attention in recent years. Pal and Das (2019) studied the combined performance of non-linear thermal radiation and chemical reaction on MHD convective heat and mass transfer of a micropolar fluid over a non-isothermal surface. Reddy and Raju (2017) studied Soret and chemical reaction effects on unsteady MHD flow of viscoelastic micropolar fluid through a porous medium with thermal radiation and heat source. Baoku and Olajuwon (2014) investigated a transient flow and mass transfer of a third grade fluid past a vertical porous plate in the presence of chemical reaction.

However, in all the references consulted to the best of our knowledge, none of the researches considered all thermophysical and chemical effects alongside reverse thermal and concentration slips (as observed in electro-osmotic flows and electrochemical systems) as being investigated in this research . The study explores studies on Soret and Dufour models as they account for the phenomenon of thermal diffusion and mass diffusion respectively; MHD model which has several applications in astrophysics, geophysics and engineering; porous medium model as it has many applications such as in ground water flow, oil and gas production, environmental remediation and bioengineering; nonlinearized thermal radiation model which has significant impact on heat transfer, especially at higher temperature like in manufacturing industries for the design of reliable equipment. These are found simultaneously on polymer and food processing; catalytic combustion in porous burners and packed-bed catalytic reactors.

Hence, the aim of the current study is to investigate the variations in the effects of these relevant thermophysical parameters on the flow, heat and mass transfer characteristics as well as on the physical quantities such as skin friction coefficient, Nusselt and Sherwood number on micropolar fluid. The present results are compared with those in the existing literature to validate the results. The highly nonlinear system of partial differential equations are solved numerically using the sixth-order Runge-Kutta scheme with shooting method. The effects of various significant parameters such as Soret number, Dufour number, chemical reaction

parameter, velocity slip, thermal slip, concentration slip, Schmidt number and others on the dimensionless temperature, velocity, angular velocity and species concentration profiles are presented graphically.

MATERIALS AND METHODS

Consider a steady, two-dimensional, hydromagnetic boundary layer flow with microrotation of heat and mass transfer of micropolar conducting and reacting fluid past a vertical linear stretching sheet with second-order slip boundary conditions in the presence of nonlinearized thermal radiation, viscous dissipation and chemical reaction of order n embedded in a Darcian porous medium. The surface temperature and species concentration of the stretching sheets inside the boundary layer are T_w and C_w respectively, where the respective stream concentration and temperature are C_∞ and T_∞. The model incorporates thermophoresis and diffusion-thermo phenomena in the heat and mass transfer analysis of the molecular and cross-heating transport as shown in Figure 1. The coordinate frame is selected such that *x*-axis is extending along the stretching sheet and *y*-axis is normal to it. The flow is assumed to be laminar with viscous incompressible micropolar fluid in which the fluid properties are assumed to be constant except for the density in the buoyancy term following the Boussinesq approximation.

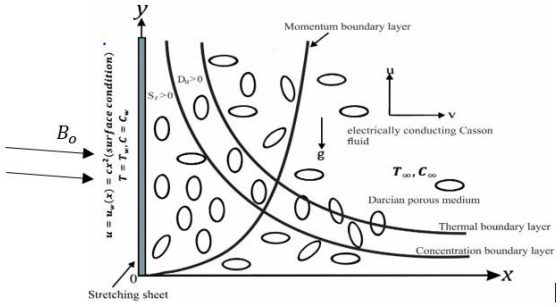

Figure 1: Flow model and coordinate system.

Under the boundary layer assumptions, the continuity, momentum, angular momentum, energy and species concentration equations can be written as follow:

$$\frac{\partial u}{\partial x} + \frac{\partial v}{\partial y} = 0 \quad (1)$$

$$u\frac{\partial u}{\partial x} + v\frac{\partial u}{\partial y} = \left(v + \frac{K^*}{\rho}\right)\frac{\partial^2 u}{\partial y^2} - \left(\frac{v}{K_1} + \frac{\sigma B_0^2}{\rho}\right)u + \frac{K^*}{\rho}\frac{\partial N}{\partial y} \quad (2)$$

$$u\frac{\partial N}{\partial x} + v\frac{\partial N}{\partial y} = \frac{\gamma}{\rho j}\frac{\partial^2 N}{\partial y^2} - \frac{K^*}{\rho j}\left(2N + \frac{\partial u}{\partial y}\right) \quad (3)$$

$$u\frac{\partial T}{\partial x} + v\frac{\partial T}{\partial y} = \frac{K}{\rho C_p}\frac{\partial^2 T}{\partial y^2} - \frac{K}{\rho C_p}\frac{\partial q_r}{K\partial y} + \frac{D_m K_T}{C_s C_p}\frac{\partial^2 C}{\partial y^2} + \frac{K^* + \mu}{\rho C_p}\left(\frac{\partial u}{\partial y}\right)^2 \quad (4)$$

$$u\frac{\partial C}{\partial x} + v\frac{\partial C}{\partial y} = D_m\frac{\partial^2 C}{\partial y^2} + \frac{D_m K_T}{T_m}\frac{\partial^2 T}{\partial y^2} - K_r\,(C - C_\infty)^n \quad (5)$$

with the following boundary conditions;

$$u = u_w + u_{slip},\ v = 0,\ N = -m\frac{\partial u}{\partial y},\ T = T_w - E\frac{\partial T}{\partial y},\ C = C_w - F\frac{\partial C}{\partial y} \quad at\ y = 0 \quad (6)$$

$$u \to 0,\quad N \to 0,\quad T \to T_\infty,\quad C \to C_\infty,\quad as\ y \to \infty \quad (7)$$

where $u_w = bx$, u and v are the velocity of fluid x-component and y-component, ν is the kinematic viscosity; K^* is the vortex viscosity, ρ is the fluid density; N is the angular velocity or microrotation, C and C_∞ are the concentration and concentration at free stream; σ is the electrical conductivity of the fluid; B_0 and K_1 are the externally imposed magnetic field strength in the y-direction and the permeability of the porous medium; γ_1 and j are the spin gradient viscosity and microrotation per unit mass; α, K, C_p and q_r are effective thermal diffusivity of the porous medium, thermal conductivity; specific heat at constant pressure and heat flux respectively; K_T, K_r and T_m are the thermal difusion ratio, chemical reaction, mean fluid temperature; C_s is the concentration susceptibility and D_m is the mass diffusivity.

Note that U_{slip} is the slip velocity at the surface is stated as employed by Lin (2008) and Ibrahim (2016)], which is given as:

$$U_{slip} = \frac{2}{3}\left(\frac{3-\alpha l^2}{\alpha}\frac{3}{2}\frac{1-l^2}{K_n}\right)\lambda_1\frac{\partial u}{\partial y} - \frac{1}{4}\left[l^4 + \frac{2}{K_n^2}(1-l^2)\right]\lambda_1^2\frac{\partial^2 u}{\partial y^2},$$

$$U_{slip} = A\frac{\partial u}{\partial y} + B\frac{\partial^2 u}{\partial y^2} \quad (8)$$

where A and B are constants, K_n is Knudsen number, $l = min\left[\frac{1}{K_n}, 1\right]$, α is the momentum accommodation coefficient with $0 \le \alpha \le 1$ and λ_1 is molecular mean free path. Regarding the definition of l, it is noticeable that for any given value of K_n, we have $0 \le l \le 1$. The molecular mean free path is always positive. Thus, it is known that < 0 , and hence the second term in the right hand side of Equation (8) a positive number.

Adopting the radiative heat flux for optically thick medium for nonlinearized Rosseland approximation as adopted by Magyari and Pantokratoras (2011) and Baoku and Falade (2019), the flow is subjected to a uniform magnetic field with strength $B = B_0$ which is applied in

the positive y −direction. Further model assumptions and representations are the following:

1. The magnetic Reynolds number is assumed to be small so that the induced magnetic field is neglected in comparison to the applied magnetic field;
2. There exerts a negligible applied electric field so that Hall effects and Joule heating are neglected;

The following similarity variable and dimensionless variables are defined as:

$$u = \frac{\partial \psi}{\partial y} = bxf'(\eta), \quad v = \frac{\partial \psi}{\partial x} = -\sqrt{b\nu} f(\eta), \quad \eta = \sqrt{\frac{a}{\nu}}\, y, \quad N = bx\sqrt{\frac{a}{\nu}}\, g(\eta). \tag{9}$$

$$\theta = \frac{(T-T_\infty)}{(T_w-T_\infty)}, \ \phi = \frac{(C-C_\infty)}{(C_w-C_\infty)} \tag{10}$$

Using Equations (9 and 10) on Equations (1) through (7), the following dimensionless system of nonlinear ordinary differential equations are obtained:

$$(1 + K_m)f''' + ff' - f'^2 - (P + M)f' + K_m g' = 0 \tag{11}$$

$$\left(1 + \frac{K_m}{2}\right)g'' + f'g - fg' - K_m(2g + f'') = 0 \tag{12}$$

$$[1 + PrR(\theta + Cr)^3]\theta'' + 3PrR(\theta + Cr)^2\theta'^2 + Prf\theta' + PrDu\phi'' + PrEc(K_m + 1)f''^2 = 0 \tag{13}$$

$$\phi'' + \mathrm{Sc}Sr\theta'' + Sc(f\phi' - \mathrm{K}_r\,\phi^n) = 0 \tag{14}$$

with the following boundary conditions;

$$f(0) = 0, \ f'(0) = 1 + Gf''(0) + L_1 f'''(0), \ g(0) = -\frac{1}{2}f''(0)$$

$$\theta(0) = 1 - \lambda\theta'(0), \quad \phi(0) = 1 - \delta\phi'(0) \quad at \quad \eta = 0. \tag{15}$$

$$f'(\infty) \to 0, \ g(\infty) \to 0, \quad \theta(\infty) \to 0, \ \phi(\infty) \longrightarrow 0 \quad as \quad \eta \to \infty. \tag{16}$$

where $Pr = \frac{\mu C_p}{\mathrm{K}}$ is the prandtl number, $Sc = \frac{\upsilon}{D_m}$ is the Schmidt number, $Du = \left(\frac{D_m \mathrm{K}_T}{\upsilon C_s C_p}\right)\left(\frac{C_w - C_\infty}{T_w - T_\infty}\right)$ is the Dufour number, $Sr = \left(\frac{D_m \mathrm{K}_T}{\upsilon T_m}\right)\left(\frac{T_w - T_\infty}{C_w - C_\infty}\right)$. is the Soret number, $P = (K^* U^2)/\upsilon^2$ is the permeability parameter, K_r is the chemical reaction parameter, $Ec = \frac{b^2x^2}{C_p(T_w - T_\infty)}$ is the Eckert number, $Cr = \frac{T_\infty}{(T_w - T_\infty)}$, is temperature ratio, λ is thermal slip parameter, δ is concentration slip parameter, G is first order slip parameter and is given by $G = A\sqrt{\frac{b}{\nu}}$, which is positive, L_1 is the second order velocity slip parameter given by $L_1 = \frac{Bb}{\nu}$ is negative, N is the microrotation, ν is the kinematic viscosity, K^* is the vortex viscosity, j is the micro-inertia density, $\Omega = \left(\mu + \frac{K^*}{2}\right)j = \mu\left(1 + \frac{K_m}{2}\right)j$, where $K_m = \frac{K^*}{\mu}$ and m is microrotation parameter which is a contact such that $0 \leq m \leq 1$; $f, g, \theta \ and \ \phi$ are the dimensionless velocity, angular velocity, temperature and concentration respectively.

The quantities of physical interest are the of skin friction coefficient, Nusselt number and Sherwood number which are defined as:

$$C_f = \frac{\tau_\omega}{\rho U_\omega^2}, \quad Nu_x = \frac{xq_\omega}{\kappa(T_\omega - T_\infty)}, \quad Sh_x = \frac{xJ_\omega}{D_m(C_\omega - C_\infty)}$$

where $\tau_\omega = [(\mu + K^*)\frac{\partial u}{\partial y} + K^* N]_{y=0}$,

$$q_\omega = -\kappa\left(\frac{\partial T}{\partial y}\right)_{y=0,} \quad J_\omega = -D_m\left(\frac{\partial C}{\partial y}\right)_{y=0}$$

Applying the above similarity transformation on the quantities of physical interest, we get:

$$Re^{1/2} = -(1 + \delta_m) \quad (1 + \tfrac{K^*}{2})f''(0), \quad Re^{-1/2}\, Nu_x = -\theta'(0), \quad Re^{-1/2}\, Sh_x = -\phi'(0)$$

where $Re_x = \frac{bx^2}{\nu}$.

Method of the Solution

In this research, Runge-Kutta-Verner (RKV) scheme of order six with shooting technique is employed to solve the coupled nonlinear system of ordinary differential equations after it has been reduced to system of first order differential equation alongside the boundary conditions. The coupled ordinary differential equations above are of third order in f, second order in g, θ and ϕ: However, since the values of f', g, θ and ϕ are known from the boundary conditions at $\eta \to \infty$; the most important part of this scheme is to determine the appropriate finite values of the solution at η_∞ which is estimated by starting with some initial guess values and solving the initial value problems consisting of equations in the model to find the appropriate values of $f''(0)$, $g'(0), \theta'(0)$, and $\phi'(0)$ corresponding to the boundary conditions. This process is repeated again by considering another value at η_∞ until two successive value of $f''(0)$, $g'(0), \theta'(0)$, and $\phi'(0)$ are obtained up to a desired significant digit to satisfy other conditions at the boundary point. In this way, the final values at $\eta \to \infty$ are obtained for a particular set of physical parameters for determining velocity $f'(\eta)$, microrotation $g(\eta)$, temperature $\theta(\eta)$ and concentration $\phi(\eta)$ in the boundary layer. Once all the nine initial conditions are known, then we can proceed to solve the system of equations by using the Runge-Kutta-Verner

integration scheme with the shooting method. The value at $\eta \to \infty$ is selected to vary depending upon a set of physical parameters in order to avoid numerical oscillations. The results are then validated with the numerical results available in the literature under some limiting cases.

Hence, the solutions, of the resulting coupled highly nonlinear equations (11) - (14) which are higher order boundary valued problems alongside the conditions (15) - (16), are available. The solutions are finalized by adjusting the initial guess based on the residual using Newton's method to refine the initial guess to shoot towards the better ends of the boundary condition as given. Below are the sets of coupled system of first order boundary value problems used for the numerical computations, which are coded into MAPLE 18 software as described by Heck (2003):

$$Z_1' = Z_2 \quad (17)$$

$$Z_2' = Z_3 \quad (18)$$

$$Z_3' = \frac{1}{(1+K_m)}[Z_2^2 - Z_1 Z_3 + (P+M)Z_2 - K_m Z_5] \quad (19)$$

$$Z_4' = Z_5 \quad (20)$$

$$Z_5' = \frac{2}{(2+K_m)}[Z_1 Z_5 - Z_2 Z_4 + K_m(2Z_4 + Z_3)] \quad (21)$$

$$Z_6' = Z_7 \quad (22)$$

$$Z_7' = \frac{1}{1+PrR(Z_6+Cr)^3}\left[\begin{matrix}-3PrR\,(Z_8+Cr)^2 Z_7^2 - PrZ_1 Z_7 - \\ PrDuZ_{11} + PrEc(1+K_m)Z_3^2\end{matrix}\right] \quad (23)$$

$$Z_9' = Z_{10} \quad (24)$$

$$Z_{10}' = -Sc(Z_1 Z_{10} - KrZ_9^n) - ScSrZ_8 \quad (25)$$

with the following initial conditions;

$$Z_1(0) = 0, \quad Z_2(0) = 1 + GZ_3(0) + L_1 Z_{31}(0), \quad Z_4(0) = -\frac{Z_3(0)}{2}$$

$$Z_6(0) = 1 - \lambda Z_7(0), \quad Z_9(0) = 1 - \delta Z_{10}(0) \quad at\ \eta = 0. \quad (26)$$

$$Z_2(\infty) \longrightarrow 0, \quad Z_4(\infty) \longrightarrow 0, \quad Z_6(\infty) \longrightarrow 0, \quad Z_9(\infty) \longrightarrow 0 \quad as\ \eta \longrightarrow \infty. \quad (27)$$

Translating the algorithm of RKV into Maple codes for several sets of emerging parameters and aforementioned sets of systems of initial value problems for the model under consideration, the step size of 0.001 is set for the computational purposes and the error tolerance of 10^{-6} is used in all the cases during coding to obtain the results.

RESULTS AND DISCUSSION

A numerical computation has been performed in order to analyze the influence of the various thermophysical parameters on the flows, heat and mass transfer of the micropolar fluid. The effects of various physical parameters on velocity, angular velocity, temperature and species concentration profiles have been discussed and shown graphically in the figures below:

Velocity Profiles

Figure 2 depicts the effect of material parameter K_m on velocity profile f', where the result shows that increasing material parameter enhances fluid velocity. Because higher viscosity reduces resistance in the porous medium, this allows easier fluid flow and increasing velocity. This corresponds to Ibrahim's result excellently. Figure 3 represents velocity profile f' for different values of magnetic field M, where it was found out that increasing magnetic field M reduces velocity f'. This observation is in line with reality as the applied magnetic field exerts Lorentz forces, which create resistance and slow down fluid motion. Moreover, Figure 4 depicts the effects of first order slip L_1 parameter on velocity profile f', where it was found out that an increase in the value of first order slip parameter L_1 leads to a slight decrease in the velocity profile f'. This observation is viewed as the slip reduces wall friction and decreasing momentum transfer near the wall in the presence of microrotation coupling in the porous space. This is also in good agreement with Ibrahim's result. However, Figure 5 shows the effect of permeability parameter P on velocity profile f, which shows that an increases in the permeability parameter P leads to a slight decrease in velocity profile f. This might be due to the fact that this increased permeability parameter restricts flow and reducing resistance to flow but the presence of strong velocity slip with opposite direction thermal slip and concentration jump might be responsible for the increased velocity boundary layer thickness.

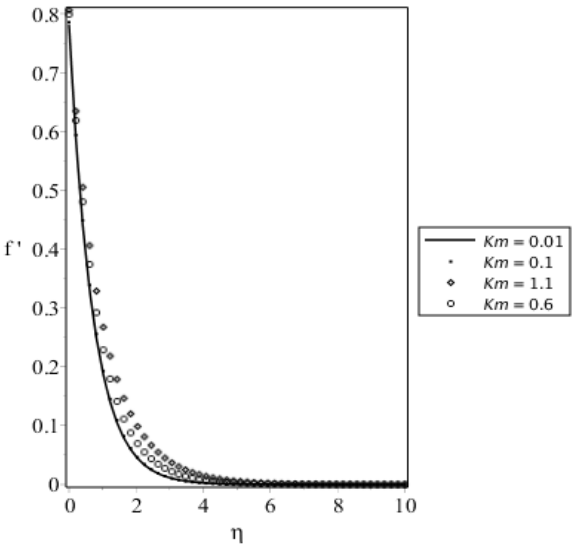

Figure 2: Velocity profile f' for different values of material parameter K_m.

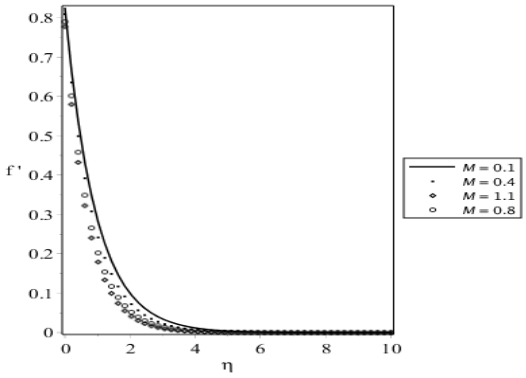

Figure 3: Velocity profile f' for different values of magnetic field M.

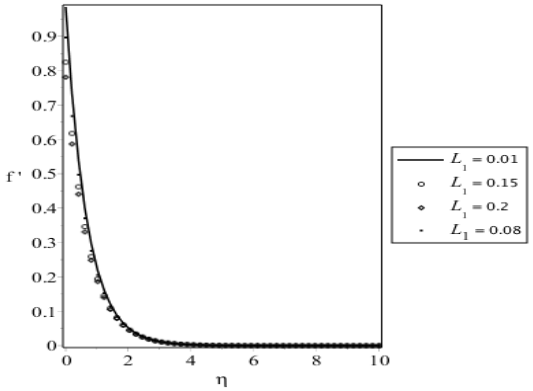

Figure 4: Velocity profile f' for different values of first order slip parameter L_1.

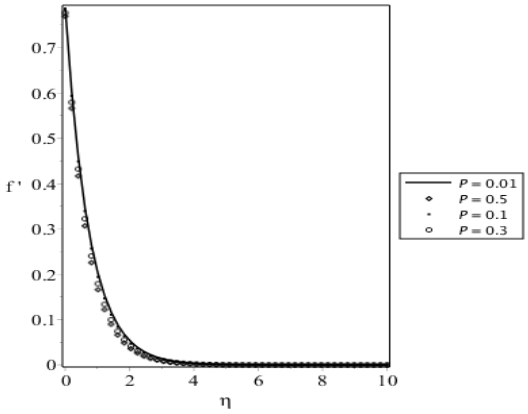

Figure 5: Velocity profile f with different value of permeability parameter P.

Angular Velocity Profiles

Figure 6 represents the effects of material parameter K_m on angular velocity g. It is observed that as the material parameter K_m increases it lead to a decreases in angular velocity parameter g. This might be due to the fact that easier flow reduce microrotation and internal resistance effects. This effect is similar to the observation of Ibrahim (11). Figure 7 depicts the effects of magnetic field parameter M on angular velocity profile g. It is noted that an increase in the values of magnetic field parameter M leads to an increases in the angular velocity profile g in this case. This might due to the influence of coupling nature of the model and hences decreases the angular velocity boundary layer thicknesses . Figure 8 shows the effect of second order slip parameter L_1 on angular velocity profile g. The result shows that an increase in the second order slip parameter L_1 leads to a decreases in angular velocity profile g, thereby increasing the microrotation boundary layer thickness. This outcome is contrary to the observation of Ibrahim (2016). The rational behind this might be is due to slip conditions reduce shear at the boundary, limiting the angular velocity. This is in confirmity with the observation of Ibrahim (2016). Figure 9 depicts the effect permeability parameter P on angular velocity profile g. The result shows that the permeability parameter P has a direct proportion effects with the angular velocity profile. This observation is in line with reality as enhancing permeability effects increases the microrotation interactions as shown even with coupling nature of the nodel.

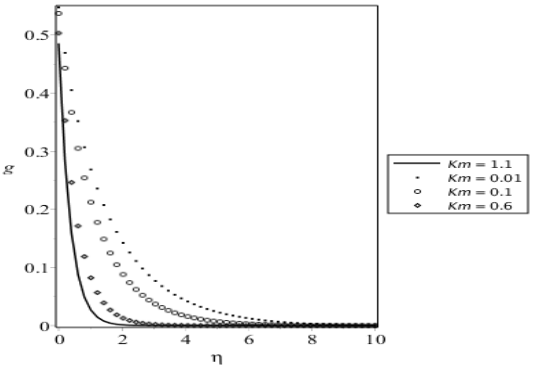

Figure 6: Angular velocity g for different value of material parameter K_m.

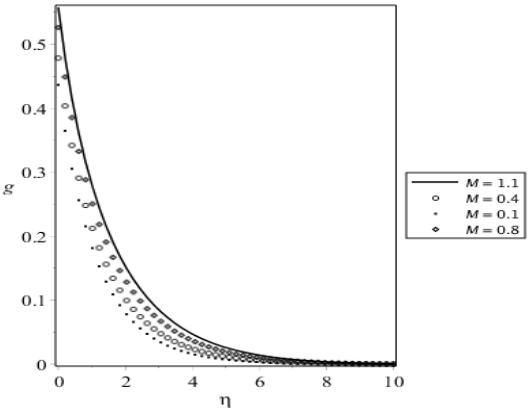

Figure 7: Angular velocity profile g for different values of magnetic field M.

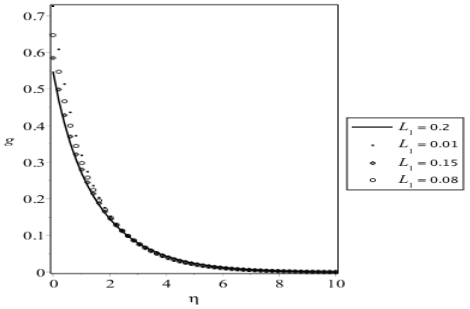

Figure 8: Angular velocity profile g with different values of first order slip parameter L_1.

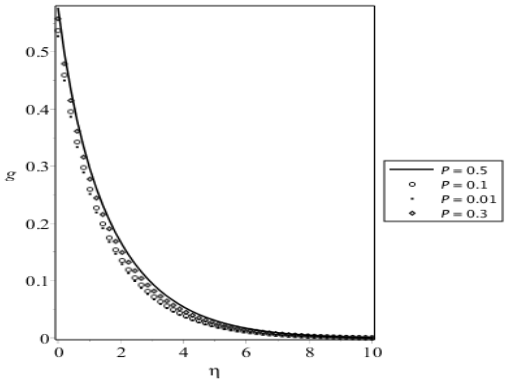

Figure 9: Angular velocity profile g with different value of permeability parameter P

It is noted that in Figures 10, there is a direct proportion in the effect between the Prandtl number Pr and fluid temperature θ. This is because the Prandtl number is directly proportional to the fluid viscosity, which enhances the temperature of micropolar fluid. Figure 11 represents the effect of first order slip parameter L_1 on temperature profile θ, it is noted that the temperatue profile increases with increases in the first order slip parameter. This is similar to the observation of Ibrahim's (2016) result. The reason might be as a result of associated thermal slip parameter enhances heat transfer, leading to an increase in temperature. Figure 12 represents the influence of chemical reaction parameter K_r on temperature profile θ, It is noticible that temperature profile θ increases with an increase in chemical reaction parameter K_r. This is be as a result of reactions often lead to release heat (exothermic), thereby raising the temperature.

Moreover, Figure 13 represents the effect of radiation parameter R on temperature profile θ. The result shows that an increases in radiation parameter R leads to an increases in temperature profile θ, This observation is in line with reality that more radiative heat energy is absorbed in the process. Figure 14 expresses the effect of temperature difference parameter Cr on fluid temperature. It is noted that an increase in the temperature difference parameter Cr leads to a decrease in temperature profile. This might be due to increase in the temperature ratio that promotes faster heat loss.

Figure 15 showcases the effect of negative thermal slip parameter λ on the fluid temperature. At the higher values of λ, the fluid temperature is enhanced with the increase in the thermal slip parameter. However, at the lower values of λ, the fluid temperature is decreased with increasing values of λ. It is also observed that the fluid temperature at the higher values of thermal slip parameter is far lower compared to that at the lower values of λ. This fluctuation confirms the nonphysical concept of negative thermal slip parameter, that only happens in exotic situations such as forced thermoelectric or active heat pumping surfaces which are rare and artificially driven.

The influence of concentration slip parameter on the fluid temperature convectionally is to impede heat transfer in the case of inherent dissipative system. In the current situation, the concentration slip parameter enhances the heat flux which leads to the increase in the fluid temperature. Hence, the negative values of concentration slip parameter enhance heat transfer spontaneously against the physical law of thermodynamics. This affirms that only in active systems could negative effective concentration slip parameters appear.

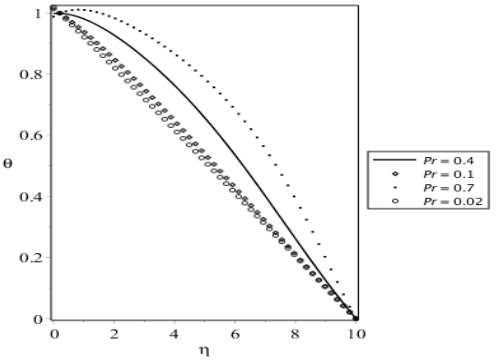

Figure 10: Temperature profile θ for different values of prandtl number Pr.

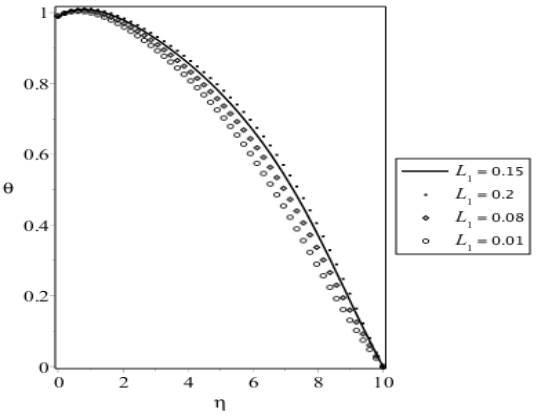

Figure 11: Temperature profile θ with different values of first order slip parameter L_1.

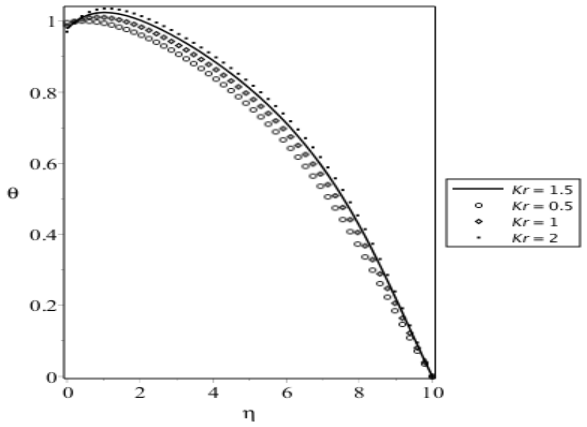

Figure 12: Temperature profile θ for different values of chemical reaction parameter K_r

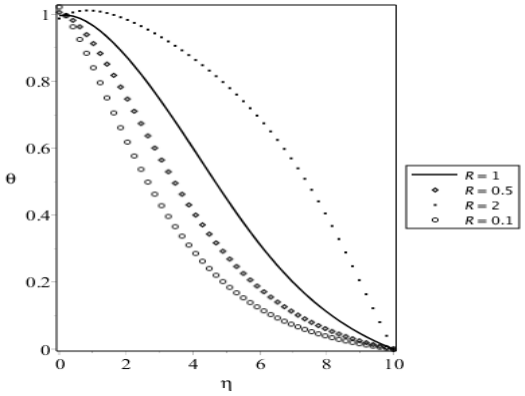

Figure 13: Temperature profile θ for different values of radiation parameter R.

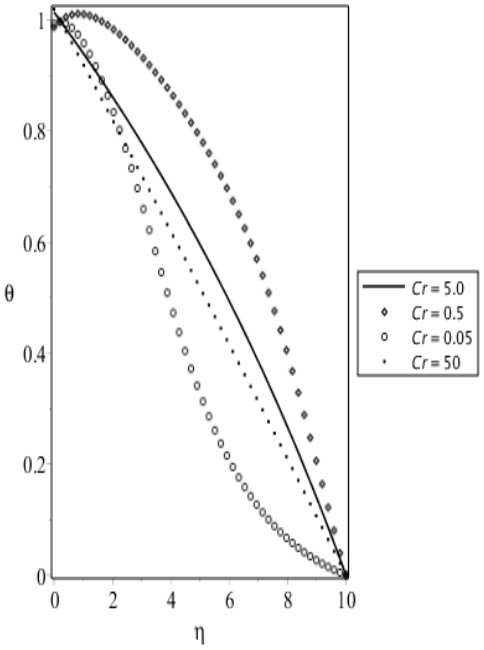

Figure 14: Temperature profile θ for different values of temperature difference parameter Cr.

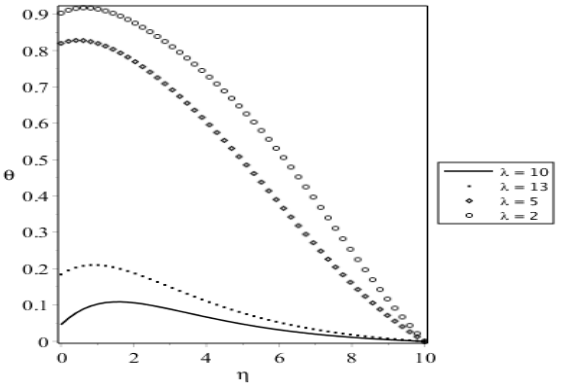

Figure 15: Temperature profile θ for different values of thermal slip parameter λ.

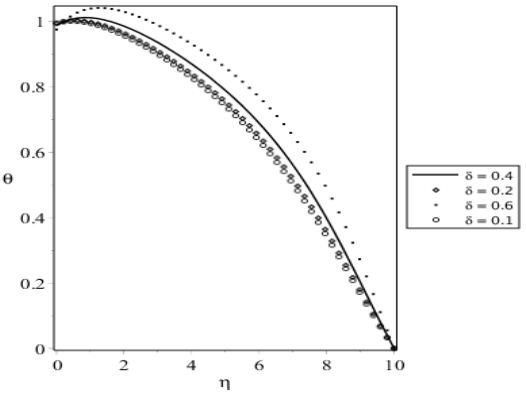

Figure 16: Temperature profile θ for different values of concentration slip parameter δ.

Species Concentration Profiles

Figure 17 depicts the effect of material parameter K_m on concentration profile ϕ. It is noted that the concentration profile decreases with the increase in material parameter slightly. This is veiwed as an increase in material parameter increases microrotation; dampens the velocity gradient and reducing convective transport of species. Figure 18 shows that the influence of Schmidt number Sc on concentration profile ϕ. The results shows that increasing the Schmidt number leads to a decreases in concentration profile ϕ. This might be due to the fact that Schmidt number reduces mass diffusivity. However, Figure 19 displays the effect of Soret number Sr on concentration profile ϕ. It is noted that the increase in Soret number Sr leads an increase in the concentration profile ϕ especially at higher values of the Soret number Sr. This observation is as a result of the temperature gradients drive species movement and raising the fluid concentration.

Moreso, Figure 20 presents the effect of order of chemical reaction parameter n on concentration profile ϕ. It is noted that the concentration profile ϕ increases with an increase in the order of chemical reaction parameter n.

This might due to complex nature of flow and reaction involved as the observation is against the expectation that higher orders of chemical reaction will exaggerate depletion, making species diffusion highly sensitive to concentration changes. Figure 21 displays the effect of concentration slip parameter λ on concentration profile ϕ. It is noted that the concentration profile ϕ increases with increases in concentration slip parameter λ. This shows that the concentration is enhanced; thereby increasing the concentration boundary layer thickness with stronger mass flux to/from the surface.

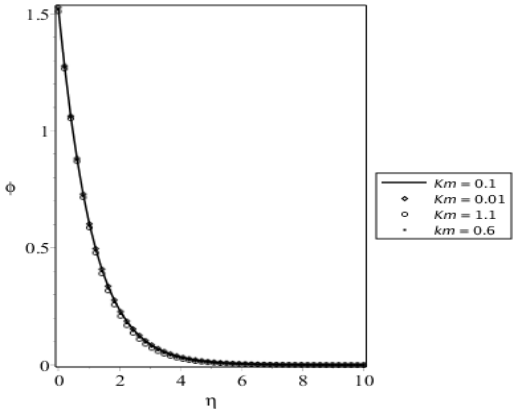

Figure 17: Concentration profile ϕ for different values of material parameter $K_{m.}$

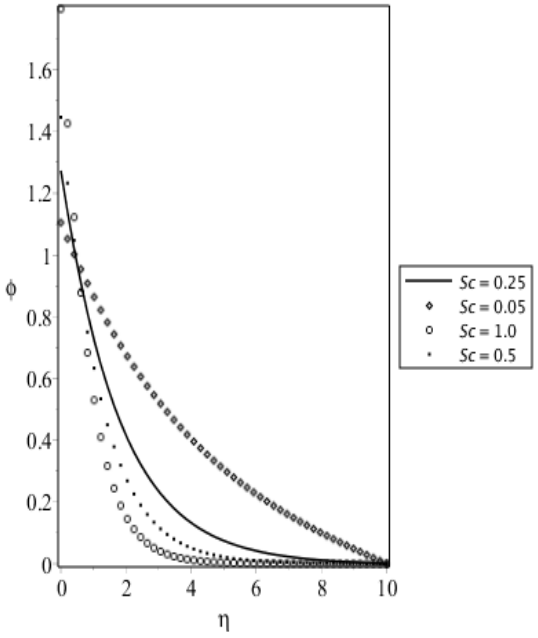

Figure 18: Concentration profile ϕ for different values of Schmidt number Sc.

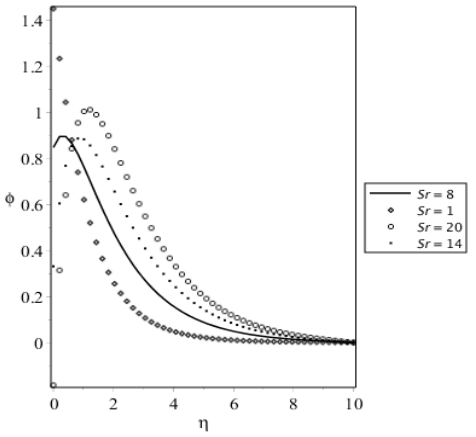

Figure 19: Concentration profile ϕ for different values of Soret number Sr.

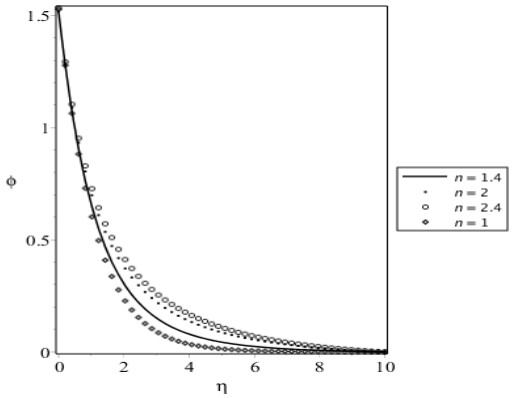

Figure 20: Concentration profile ϕ for different values of order of chemical reaction n.

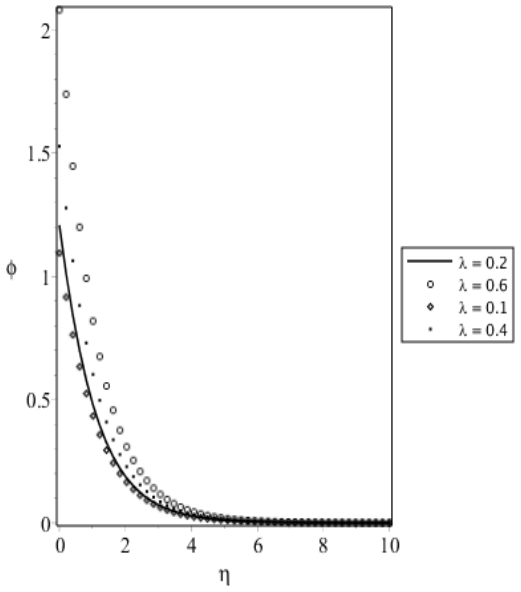

Figure 21: Concentration profile ϕ for different values of thermal slip parameter λ.

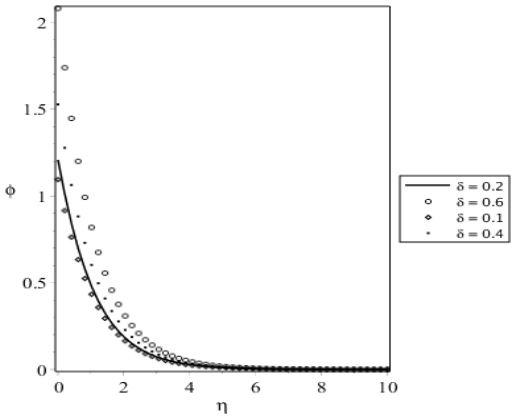

Figure 22: Concentration profile ϕ for different values of concentration slip parameter δ.

Table 1 and 2 shows the values of skin-friction, local Nusselt and Sherwood numbers for various values of some selected parameters. It is noted that an increase in the material parameter results to unstable solution for skin-friction coefficient and heat transfer coefficient, but increase in the rate of mass transfer. Decreases in magnetic field parameter results to decreases in skin-friction coefficients and it increases in rate of heat transfer. Decreases in porous medium parameter correspond to a decreases in skin-friction coefficient and heat transfer's rate but increase in rate of mass transfer. It is also noted that a decrease in Prandtl and Soret numbers results in decreases on skin-friction coefficient, rate of heat transfer, whereas the reverse effect is recorded on rate of mass transfer. Validation to ensure the accuracy of the current numerical is expressed in Table 3. In Table 3, the results of the current method (Runge-Kutta-Verner) are compared with those of Ibrahim (2017) who employed bvp4c of MATLAB; the latter is a finite difference numerical approach that provides continuous solutions that are of fourth order. The comparison of the two methods was found to be in very good agreement.

Table 1: Numerical computations showing the physical quantities of interest: $-f''(0)$, $-\theta'(0)$ and $-\phi'(0)$.

K	G	Pm	λ	n	$-f''^{(0)}$	$\theta(0)$	$-\theta'(0)$	$\phi(0)$	$-\phi'(0)$
0.01	0.2	0.2	0.2	1	1.0955	0.9875	0.0626	1.5274	1.3185
0.1	0.2	0.2	0.2	1	1.0748	0.9851	0.0745	1.5262	1.3155
1.0	0.2	0.2	0.2	1	1.0955	0.9782	0.0499	1.5126	1.2913
0.01	0.01	0.2	0.2	1	1.4523	0.9912	0.0437	1.5418	1.3545
0.01	0.02	0.2	0.2	1	1.4270	0.9875	0.0449	1.5274	1.3521
0.01	0.06	0.2	0.2	1	1.3351	0.9901	0.0494	1.5373	1.3433
0.01	0.2	0.2	0.4	1	1.0955	0.9876	0.0605	1.5274	1.3185
0.01	0.2	0.2	0.6	1	1.0955	0.9648	0.0587	1.5274	1.3185
0.01	0.2	0.2	0.8	1	1.0955	0.9545	0.0569	1.5274	1.3185
		0.4			1.1355	0.9877	0.0618	1.5247	1.3118
		0.5			1.1546	0.9877	0.0613	1.5235	1.3087
		0.52			1.1583	0.9877	0.0612	1.5233	1.3081
				1.3	1.0955	0.9888	0.0561	1.5169	1.2923
				1.6	1.0955	0.9896	0.0522	1.5127	1.2818
				2.0	0.9773	0.9900	0.0856	1.5165	1.2483

Table 2. Numerical computations showing the physical quantities of interest; $-f''^{(0)}$; $\theta'(0)$ and $-\phi'(0)$.

M	Pr	δ	Sr	Du	$-f''(0)$	$\theta(0)$	$-\theta'(0)$	$\phi(0)$	$-\phi'(0)$
0.3	0.71	0.4	0.1	0.2	0.9303	0.9878	0.0612	1.5396	1.3489
0.4	0.71	0.4	0.1	0.2	0.9569	0.9876	0.0620	1.5375	1.3436
0.5	0.71	0.4	0.1	0.2	0.9823	0.9875	0.0625	1.5355	1.3388
1	0.71	1.5	0.1	0.2	1.0955	1.0301	0.1506	-3.1725	2.7817
1	0.71	2.0	0.1	0.2	1.0955	1.0186	0.0929	-1.3051	1.1525
1	0.71	2.5	0.1	0.2	1.0955	1.0149	0.0745	-0.8171	0.7268
	0.2				1.0955	1.0069	0.0342	1.5274	1.3185
	0.4				1.0955	0.9984	0.0081	1.5274	1.3185
	0.5				1.0955	0.9948	0.0262	1.5274	1.3185
			0.01		1.0955	0.9871	0.0644	1.5351	1.3378
			0.02		1.0955	0.9872	0.0642	1.5343	1.3357
			0.03		1.0955	0.9872	0.0640	1.5334	1.3335
			0.1	-1	1.0955	1.0489	0.2446	1.5274	1.3185
				-2	1.0955	1.0714	0.3571	1.5274	1.3185
				-3	1.0955	1.0883	0.4420	1.5274	1.3185

Table 3: Comparisons of $-f''^{(0)}$ and $\theta'(0)$ with Ibrahim W. (2017) for various values of γ and Pr at $M = 0$, $\delta = 0$ and $\beta = 0$.

γ	Ibrahim $-f''(0)$	Present result $-f''(0)$	Pr	Ibrahim $-\theta'(0)$	Present result $-\theta'(0)$
1	0.4302	0.4302	0.72	0.4636	0.4636
2	0.2840	0.2840	1	0.5822	0.5820
3	0.2141	0.2141	3	1.1652	1.1652

CONCLUSION

The study focuses on heat and mass transfer of a magnetohydrodynamic boundary layer micropolar fluid flow with multiple slip effects in a porous medium; considering diffusion-thermo and thermal-diffusion effects in the presence of nonlinearized thermal radiation and nth chemical reaction. The research x-rays the phenomena as experienced in electro-osmotic flows and electrochemical systems where temperature and concentration jumps happened in opposite direction and their values are taken to be negative. After non-dimensionalization of the boundary layer equations for the model, the resulting highly nonlinear system of ordinary differential equations are solved numerically using the sixth-order Runge-Kutta-Verner integration scheme with shooting method. The effects of various significant parameters on the dimensionless velocity, angular velocity, temperature and species concentration profiles are presented graphically. This study successfully demonstrates that thermophysical and chemical parameters (especially thermal and concentration slip) significantly influence micropolar fluid behaviour. Key findings include:

- It was found out that the magnetic field, first order slip and porous medium parameters reduce the fluid velocity, whereas the material parameter has opposite effects for the velocity;
- It is also observed that the magnetic field, Prandtl number, first order slip, Schmidt number, chemical reaction, radiation, Dufour number, concentration slip and porous medium parameters increase the fluid's temperature, whereas the reverse effects are recorded on permeability, Soret number, temperature difference and thermal slip parameters;
- It is further noted that an increase in the material parameter results to decrease on skin-friction coefficient and rate of heat transfer, but increase in the rate of mass transfer;

A decrease in magnetic field and porous medium results to decreases in skin-friction coefficient and increases in the rate of heat transfer, but in case of mass transfer's rate the reverse effect is recorded.

REFERENCES

ABDULAZIZ, O. AND HASHIM, I. (2009). Fully Developed Free Convection Heat and Mass Transfer of a Micropolar Fluid between Porous Vertical Plates. *Numerical Heat Transfer*, Part A, 55, 270–288. doi.org/10.1080/10407780802628961

ABEL, S. M., AND NANDEPPANAVAR, M. M. (2009). Heat Transfer in MHD Viscoelastic Boundary Layer Flow Over a Stretching Sheet with Non-uniform Heat Source/Sink. *Commun Nonlinear Sci*

Numer Simulat 14(5), 2120–2131, doi:10.1016/j.cnsns.2008.06.004

BAOKU, I. G., ISRAEL-COOKEY, C. AND OLAJUWON B. I. (2010). Magnetic Field and Thermal Radiation Effects on Steady Hydromagnetic Couette Flow through a Porous Channel. *Survey in Mathematics and its Applications*, 5, 215-228.

BAOKU, I. G. AND FALADE, K. I. (2017): MHD Mixed Convective Flow of a Second Grade Fluid in the Presence of Nonlinearized Thermal Radiation, Thermal Diffusion and Diffusion-thermo Effects. *Nigerian Journal of Mathematics and Applications*, 26, 173 - 190.

BAOKU, I. G. AND OLAJUWON, B. I. (2014). Transient Flow and Mass Transfer of a Third Grade Fluid past a Vertical Porous Plate in the Presence of Chemical Reaction. *Nigerian Journal of Science*, 48, 47 – 56.

BHATTACHARYYA, K., MUKHOPADHYAY, S., LAYEK G. C. AND POP, L. (2012). Effects of Thermal Radiation on Micropolar Fluid Flow and Heat Transfer over a Porous Shrinking Sheet. *International Journal of Heat and Mass Transfer* 55, 2945–2952. https://doi.org/10.1016/j.ijheatmasstransfer.2012.01.051

CHEN, X., YANG, W., ZHANG, X. AND LIU, F. (2019). Unsteady Boundary Layer Flow of Viscoelastic MHD Fluid with a Double Fractional Maxwell Model. *Applied Mathematics Letters* 95, 143–149. doi.org/10.1016/j.aml.2019.03.036

CHENG, Y. C. (2006). Fully Developed Natural Convection Heat and Mass Transfer of a Micropolar Fluid in a Vertical Channel with a Symmetric Wall Temperatures and Concentrations. *International Communications in Heat and Mass Transfer*, 33, 627-635. doi.org/10.1016/j.icheatmasstransfer.2006.01.014

ERINGEN, A. C. (1966). Theory of Micropolar Fluids. *Journal of Mathematics and Mechanics* 16, 1–18.
HECK, A. (2003). Introduction to Maple, 3rd Edition, Springer-Verlag, Germany.

IBRAHIM, W. (2017). MHD Boundary Layer Flow and Heat Transfer of Micropolar Fluid past a Stretching Sheet with Second-order Slip. *The Brazilian Society of Mechanical Sciences and Engineering*, 39, 791-799. doi:10.1007|540430.016.0621-8

LIN, W. (2008). A Slip Model for Rarefied Gas Flows at arbitrary Knudsen Number. *Appl. Phys. Lett.* 93, 253103. doi.org/10.1063/1.3052923

MAHANTESH, M., NANDEPPANAVAR, K. VAJRAVELU AND SUBHAS, M. A. (2011). Heat Transfer in MHD Viscoelastic Boundary Layer Flow over a Stretching Sheet with Thermal Radiation and Non-uniform Heat Source/Sink. *Commun. Nonlinear Sci. Numer Simulat*, 16(9), 3578–3590. doi:10.1016/j.cnsns.2010.12.033

MAGYARI, E. AND PANTOKRATORAS, A. (2011). Effect of Thermal Radiation in the Linearized Rosseland Approximation on the Heat Transfer Characteristics of various Boundary Layer Flows. *International Communication in Heat and Mass Transfer*; 38, 554- 556. doi.org/10.1016/j.icheatmasstransfer.2011.03.006

MIRGOLBABAEE, H., LEDARI, S. T. AND GANJI, D. (2017). Semi-Analytical Investigation on Micropolar Fluid Flow and Heat Transfer in a Permeable Channel using AGM. *Journal of the Association of Arab.* 24, 213-222. doi.org/10.1016/j.jaubas.2017.01.002.

PAL, D. AND DAS, B. C. (2021). Soret-Dufour Magneto-Thermal Radiative Convective Heat and Mass Transfer of Chemically and Thermally Stratified Micropolar Fluid over a Vertical Stretching/Shrinking Surface in a Porous Medium. *International Journal for Computational Methods in Engineering Science and Mechanics.* 22, 410-424. doi.org/10.1080/15502287.2021.1889073.

PAL, D. AND DAS, B. C. (2019). Combined Performance of Non-linear Thermal Radiation and Chemical Reaction on MHD Convective Heat and Mass Transfer of a Micropolar Fluid over a non isothermal surface. *International Journal of Ambient Energy*, *43*(1), 8–20. https://doi.org/10.1080/01430750.2019.1613675

PAL, D. AND DAS, B. C. (2019). Combined Performance of Non-linear Thermal Radiation and Chemical Reaction on MHD Convective Heat and Mass Transfer of a Micropolar Fluid over a Non-isothermal Surface. *International Journal of Ambient Energy.* 43, 8-20. doi.org/10.1080/01430750.2019.1613675.

REDDY, D.B. AND RAJU, G.S.S. (2017). Soret and Chemical Reaction Effects on Unsteady MHD Flow of Viscoelastic Micropolar Fluid Through a Porous Medium with Thermal Radiation and Heat Source.

Journal of Mathematics, 13, 70-84. doi: 10.9790/5728-1302037084

SUI, J., ZHAO, P., CHENG, Z. AND DOI, M. (2017). Influence of Particulate Thermophoresis on Convection Heat and Mass Transfer in a Slip Flow of a Viscoelasticity-Based Micropolar Fluid. *International Journal of Heat and Mass Transfer* 119, 40–51. doi.org/10.1016/j.ijheatmasstransfer.2017.11.104

Vijaya Lakshmi, R., Sarojamma, G., Sreelakshmi, K., Vajravelu, K. (2019). Heat Transfer Analysis in a Micropolar Fluid with Non-Linear Thermal Radiation and Second-Order Velocity Slip. In: Rushi Kumar, B., Sivaraj, R., Prasad, B., Nalliah, M., Reddy, A. (eds) Applied Mathematics and Scientific Computing. Trends inMathematics.Birkhäuser,Cham.doi.org/10.1007/978-3-030-01123-9_38